K-shell ionization of elements Ca to Zn for 0.5 to 2.5-MeV/amu ^{14}N-ion bombardment*

F. D. McDaniel and J. L. Duggan
Department of Physics, North Texas State University,† Denton, Texas 76203

P. D. Miller and G. D. Alton
Oak Ridge National Laboratory, Oak Ridge, Tennessee 37830

(Received 14 October 1976)

Target K-shell x-ray production cross sections, x-ray energy shifts, and $K\beta/K\alpha$ ratios have been measured for 7–35-MeV ^{14}N ions on thin solid films of Ca, Ti, V, Cr, Mn, Fe, Co, Ni, Cu, and Zn. Comparisons of the data were made with theoretical predictions obtained from the binary-encounter approximation and the plane-wave born approximation (PWBA). These theories were found to overpredict the experimental data by a factor of 10 at the lower energies. However, at the lower energies, the PWBA, with modifications for increased target electron binding, Coulomb deflection, target electron polarization, and relativistic effects produced results in good agreement with the experimental data. At higher energies, a systematic deviation of the theoretical predictions from the experimental data was found which increases as the ratio of Z_1/Z_2 becomes larger. Corrections to the fluorescence yields attributable to multiple ionization processes and the addition of electron capture contributions to the previously indicated direct ionization theories produced results in excellent agreement with the experimental data with the exception of those for the light elements at the highest energies.

I. INTRODUCTION

During the past few years, considerable effort has been devoted to the study of inner-shell ionization produced in ion-atom collisions. Two primary types of inner-shell excitation mechanisms have been considered; (1) direct Coulomb excitation[1] between the incident ion and the electron, and (2) electron promotion[2] due to the formation of quasimolecular orbitals during the collision. These excitation mechanisms are believed to be appropriate for certain ranges[3] of the parameters Z_1/Z_2 and v_1/v_e, where Z_1 and Z_2 are projectile and target nuclear charges, respectively, v_1 and v_e are projectile velocity and the mean target electron velocity, respectively. For $Z_1/Z_2 \ll 1$ and $v_1/v_e \gtrsim 1$, Coulomb ionization is expected to be dominant, while for $Z_1 \sim Z_2$ and $v_1/v_e \ll 1$, electron promotion should be the principal interaction mechanism.[1]

Classical and quantum-mechanical theoretical approaches have been employed to calculate Coulomb ionization probabilities. The primary Coulomb ionization models which have been used are the binary-encounter approximation (BEA) developed by Garcia *et al.*,[4] and the plane-wave Born approximation (PWBA) developed by Merzbacher *et al.*[5] Both approaches have been reasonably successful for proton bombardment of heavy elements.[6] However, for ^{4}He and ^{7}Li incident ions,[7,8] both the BEA and the PWBA have been found to overpredict the experimental x-ray cross sections at incident ion energies of the order of a few MeV.

Basbas, Brandt, and Laubert have modified the PWBA by including effects due to Coulomb deflection of the incident ion by the target nucleus and to increased binding of the target electrons due to penetration of the K shell by the projectile.[9] These modifications have removed some of the discrepancy between theory and experiment at the lower velocities.[7,8] Further modifications to the PWBA by Basbas *et al.*[10–12] include the effects due to polarization of the target electron wave function by high-velocity incident ions.[10–13] These modifications to the PWBA for increased target binding energy, Coulomb deflection of the projectile, and polarization have produced results in good agreement with the experimental cross sections for both ^{14}N (Ref. 14) and ^{16}O bombardment (Ref. 15). For heavier target systems, relativistic effects, which were expected to be important by Jamnik and Zupancic[16] as well as others[17,18] have indeed been observed to be an important consideration for both ^{7}Li (Ref. 8) and ^{14}N bombardment (Ref. 14). In short, for projectile target combinations such that $Z_1/Z_2 \ll 1$, the PWBA with the indicated modifications can be used to provide good predictions of the experimental x-ray cross sections.

For heavier projectiles at intermediate velocities such that $Z_1/Z_2 < 1$ and $v_1/v_e < 1$, experimental[19,20] and theoretical[21] results indicate that K-electron transfer to bound states of the projectile may be very important in target K-vacancy production. In fact, for projectiles initially having K vacancies, this may be the dominant mechanism.[22,23] For heavier projectiles at low and intermediate velocities such that $Z_1/Z_2 \lesssim 1$ and $v_1/v_e < 1$, Meyerhof *et al.*[24] have observed that

K-vacancy sharing between the projectile and target is larger than simple Coulomb ionization by orders of magnitude. For heavier projectiles at higher velocities such that $Z_1/Z_2 \lesssim 1$ and $v_1/v_e > 1$, recent experiments by Cue *et al.*[25] indicate that charge transfer is not important in K-vacancy production and Coulomb ionization again dominates.

The purpose of the present investigation is to determine x-ray production in a region of the parameters Z_1/Z_2 and v_1/v_e where Coulomb ionization should be the dominant excitation mechanism. In particular, measurements have been made of x-ray production cross sections, energy shifts, and $K\beta/K\alpha$ ratios for ^{14}N ions on thin targets of Ca, Ti, V, Cr, Mn, Fe, Co, Ni, Cu, and Zn. In the present work the ranges of the parameters Z_1/Z_2 and v_1/v_e lie between $0.23 \leq Z_1/Z_2 \leq 0.35$ and $0.17 \leq v_1/v_e \leq 0.58$, respectively. The experimental x-ray production cross sections are compared to the theoretical predictions obtained from the BEA, the PWBA, the PWBA with Coulomb deflection and binding energy corrections (PWBA-BC), the PWBA-BC with polarization corrections (PWBA-BCP), and the PWBA-BCP with an approximate correction for relativistic effects (PWBA-BCPR). In addition to direct ionization mechanisms, the contributions to the cross section due to electron capture are included. Preliminary portions of this study have been presented earlier.[26]

II. EXPERIMENTAL PROCEDURES

Nitrogen ions of energy from 7 to 35 MeV were obtained from the Tandem Van de Graaff accelerator at Oak Ridge National Laboratory. The incident charge states of the ions were 3+, 4+, or 5+ and were selected by the energy of interest. The experimental procedures have been discussed in detail earlier[8] and will only be briefly presented here. The ion beam was collimated by two Ta apertures 1 mm in diameter, and separated by 30 cm. The ion beam was also passed through a C aperture approximately 3 cm in front of the target to minimize small-angle scattering of the ion beam from the Al target frames. Thin transmission targets which were vacuum deposited on 10-50 μg/cm^2 carbon backings were mounted at 45° with respect to the incident beam direction. The target thicknesses are given in Table I. X rays were detected by an ORTEC Si(Li) detector, 6 mm in diameter, with a 0.00076-cm Be window. The detector was positioned inside the scattering chamber at 90° to the incident beam direction. The resolution of the Si(Li) detector was 170 eV at 5.9 keV. A 0.01-cm Mylar absorber was positioned between the target and the detector to reduce contributions to the counting rate from low-energy photons from the L-shell radiations. The absolute efficiency of the Si(Li) detector was determined by standard techniques[27] and has been discussed earlier.[7,8]

TABLE I. Target thicknesses.

Element	Z	Thickness[a] (μg/cm^2)
Ca	20	28.7
Ti	22	15.8
V	23	17.6
Cr	24	12.3
Mn	25	79.7
Fe	26	16.4
Co	27	21.2
Ni	28	80.7
Cu	29	55.6
Zn	30	66.8

[a] Actual target thickness at 45°.

The elastically scattered ^{14}N ions, which were monitored simultaneously with the x-ray spectra in Si surface barrier detectors positioned at 30° and 45°, were expected to be Rutherford in nature.[28] The scattering of ^{14}N ions was also checked by scattering them from a 100-μg/cm^2 Au foil mounted in a second target chamber positioned directly behind the primary chamber. A Si surface barrier detector, mounted at 90° with respect to the incident beam direction in the second scattering chamber, monitored the ^{14}N ion scattering from the Au target. The ratio of scattered ^{14}N ions from the target foil to those from the Au foil was a constant for each target as a function of incident ion energy, and therefore ^{14}N scattering from all targets investigated were Rutherford in nature. The solid angles subtended by the detectors were determined with a calibrated ^{244}Cm alpha-particle source.

III. DATA ANALYSIS

X-ray production cross sections were determined from the expression

$$\sigma_{Kx}(E) = \left(\frac{Y_{K\alpha}}{\epsilon_{K\alpha}} + \frac{Y_{K\beta}}{\epsilon_{K\beta}}\right)\sigma_R(E, \theta)\,\frac{d\Omega_R(\theta)}{Y_R(E, \theta)}\,\tau_{DT}T\,, \qquad (1)$$

where $Y_{K\alpha}$ and $Y_{K\beta}$ are the yields of $K\alpha$ and $K\beta$ x rays, respectively; $\epsilon_{K\alpha}$ and $\epsilon_{K\beta}$ are the Si(Li) detector efficiencies at the observed $K\alpha$ and $K\beta$ x-ray energies; $\sigma_R(E, \theta)$ is the Rutherford differential cross section at ion energy E, and scattering angle θ; $d\Omega_R(\theta)$ is the particle detector solid angle; $Y_R(E, \theta)$ is the yield of scattered ^{14}N ions; τ_{DT} is the electronic dead-time correction for both the x-ray and scattered ion yields; and T is a correction factor for energy loss in a particular thin foil.

The correction T, described by Laubert *et al.*,[29] is an approximate correction to both the x-ray and scattered ion yields for energy loss of the ions in passing through finite target thicknesses. For the 80-μg/cm^2-thick Mn target described in Table I, the combined correction to the x-ray and scattered ion yields was 2% at the highest energy and 18% at the lowest energy. Target x-ray self-absorption was estimated for the lowest x-ray energies and found to be less than 0.4%. Equation (1) assumes isotropy of x-ray emission induced by charged-particle bombardment, which has been verified by a number of different workers.[30]

Recoil effects[31-34] in x-ray cross-section measurements are expected to be negligible until $Z_1 \gtrsim Z_2$ and then only for small values of the direct ionization cross section.[34] A simple estimate of the magnitude of recoil effects produced by ^{14}N ion bombardment of Ca indicates that the contribution to the Ca K x-ray yield from recoiling Ca +Ca collisions is less than 1% of that produced by ^{14}N +Ca collisions.

In addition, x-ray energy shifts and $K\beta/K\alpha$ ratios were also determined. Absolute energy shifts were obtained by comparison of the target x-ray energy observed from ^{14}N ion bombardment with an energy calibration determined with radioactive sources and periodically checked at each ion energy.

IV. THEORETICAL CALCULATIONS

The PWBA and PWBA-BC calculations were made after prescriptions given by Basbas, Brandt, and Laubert.[9,10] The K-shell ionization cross section in the PWBA formalism is given[9,10] by

$$\sigma_K^{\mathrm{PWBA}} = (\sigma_{0K}/\theta_K) F(\eta_K/\theta_K^2), \tag{2}$$

where

$$\sigma_{0K} = 8\pi a_0^2 (Z_1/Z_{2K})^2, \tag{3}$$

$$\theta_K = U_K/Z_{2K}^2 R, \tag{4}$$

$$Z_{2K} = Z_2 - 0.3, \tag{5}$$

$$\eta_K = v_1^2/(Z_{2K} v_0)^2 = (\theta_K/2)^2 \xi_K^2. \tag{6}$$

In the previous expressions, θ_K is the reduced binding energy, η_K is the reduced particle velocity parameter, ξ_K is the universal projectile velocity parameters, Z_1 and Z_2 are the nuclear charges of the projectile and target, respectively, a_0 is the Bohr radius, U_K is the K-shell binding energy, R is the Rydberg constant, v_1 is the projectile velocity, and v_0 is the Bohr velocity. F is a tabulated[35,9] universal function of η_K and θ_K, and was calculated from an analytical expression given by Brandt and Lapicki.[36] Basbas *et al.* have introduced corrections to the PWBA for Coulomb deflection of the projectile and increased target electron binding energy due to penetration of the K shell by the projectile.[9,10] The PWBA modified to include these corrections (PWBA-BC) is given by

$$\sigma_K^{\mathrm{PWBA\text{-}BC}} = 9E_{10}(b\epsilon\theta_K\eta_K^{-3/2})(\sigma_{0K}/\epsilon\theta_K) F(\eta_K/\epsilon^2\theta_K^2), \tag{7}$$

where E_{10} is an exponential integral of order 10, b is a constant for a particular projectile-target combination, and ϵ is the binding-energy correction factor. The first factor incorporates the correction for Coulomb deflection. The binding energy correction is incorporated by replacing θ_K by $\epsilon\theta_K$ with $\epsilon \geq 1$. The inclusion of the binding energy correction factor, ϵ, produces values of $\epsilon\theta_K$ which exceed those tabulated by Khandelwal, Choi, and Merbacher.[35] The $\epsilon\theta_K$ are used to determine the value of the universal function, $F(\eta_K/\epsilon^2\theta_K^2)$, in the PWBA-BC calculation. For the present work, all theoretical calculations of the PWBA-BC cross sections for incident ion energies < 30 MeV would have to be made from values of the universal function, $F(\eta_K/\epsilon^2\theta_K^2)$, obtained by extrapolation from the table. The uncertainty in the theoretical calculations that such an extrapolation introduces will most likely depend upon the extrapolation procedure used and could possibly be quite significant. For the present data, the values of the universal function used to determine the PWBA cross sections were calculated from an approximate analytic expression given by Brandt and Lapicki.[36] The theoretical values of the PWBA-BC determined from the analytical expression were compared directly with those calculated by Basbas[10] using extrapolated values of the universal function, F. The two calculations were in excellent agreement at lower incident-ion energies (< 20 MeV). At higher incident-ion energies (> 20 MeV), the analytic function calculations were slightly lower in magnitude than those obtained by the extrapolation. For the present work the differences are negligible at 7 MeV and approach 10% at 35 MeV.

Further modifications to the PWBA by Basbas *et al.*[10-12] include effects attributed to polarization of the target electron wave function by the high-velocity incident ions. This high-velocity polarization effect is believed to decrease the effective interaction distance between the incident ion and the target electron through a distortion of the electronic orbit which results in a decrease in the electron binding energy and an increase in the ionization probability. The polarization effect is incorporated in the PWBA by Basbas *et al.*[10] by a further modification of the reduced binding energy, θ_K. In this approach, θ_K is replaced by $\zeta\theta_K$ which

includes binding energy and polarization effects. The PWBA with binding energy, Coulomb deflection, and polarization corrections (PWBA-BCP) is given by

$$\sigma_K^{\text{PWBA-BCP}} = 9E_{10}(b\zeta\theta_K\eta_K^{-3/2})(\sigma_{0K}/\zeta\theta_K)F(\eta_K/\zeta^2\theta_K^2). \quad (8)$$

At low incident-ion energies for the heavier targets relativistic effects are expected to be important.[16-18] Relativistic corrections, which are expected to increase the theoretical cross sections, were incorporated through an approximate correction due to Hansen.[18] This correction consists of a multiplicative factor to the BEA cross section. This correction has been made to the PWBA cross sections in the present work.

The PWBA, with modifications for increased binding energy, Coulomb deflection, polarization, and relativistic effects is labeled PWBA-BCPR. Table II presents calculated cross sections at two energies of interest using the PWBA with and without modifications for Coulomb deflection (C), increased binding (B), polarization (P), and relativistic effects (R). One observes that the correction for Coulomb deflection of the heavy ^{14}N ion is quite small in comparison to the binding-energy correction which is very large. The polarization corrections are greater at higher velocities and for larger values of Z_1/Z_2. Relativistic corrections are more important at lower incident-ion velocities for heavier target elements.

The BEA calculations are made according to prescriptions given by McGuire and Richard.[37] It is not clear that the BEA, modified to include corrections for Coulomb deflection[38] and increased electron binding, would not represent the ionization process as well as that obtained by the modified PWBA.

V. RESULTS AND DISCUSSION

The results of the present investigation are presented in Table III. The uncertainties associated with the x-ray production cross sections have been discussed earlier[8] and range from 7–10%. The uncertainties in the $K\beta/K\alpha$ ratios are due primarily to statistical uncertainties in the x-ray yields and backgrounds, and range from 6–10%. The uncertainties in the $K\alpha$ and $K\beta$ energy shifts are due primarily to the uncertainty in the location of the x-ray peak centroids and the stability of the Si(Li) detector and amplifier. These uncertainties have been estimated to be <10 and <20 eV, respectively. The present measurements are in excellent agreement with the recent data of Gray *et al.*[39] for ^{14}N ions on thin Ni targets.

It was found earlier[7] that the theoretical predictions of the PWBA, with corrections for Coulomb deflection of the projectile and increased target electron binding energy (PWBA-BC) underestimated the experimental cross sections by $\simeq 10\%$ for 0.5–2.5 MeV ^{4}He bombardment in the range of elements from $22 \leq Z_2 \leq 39$.

TABLE II. PWBA K-shell x-ray production cross sections with and without modifications for Coulomb deflection, increased binding, polarization, and relativistic effects. Cross sections are in units of barns.

	$_{20}$Ca $\omega_0 = 0.163$		$_{30}$Zn $\omega_0 = 0.479$	
	7 MeV	35 MeV	7 MeV	36 MeV
PWBA	1303	20360	49.4	3238
PWBA-C	1250	20290	43.2	3201
PWBA-B	58.0	10690	2.26	1030
PWBA-BC	54.3	10650	1.85	1015
PWBA-BCP	63.0	18080	1.87	1297
PWBA-BCPR	64.7	18240	2.27	1335

For ^{7}Li ion bombardment of elements $22 \leq Z_2 \leq 51$ in the energy range from 7–35 MeV, the PWBA-BC (with approximate relativistic corrections included for the heavier target species) underestimated the experimental cross sections by $\simeq 10\%$ at lower ion energies and $\leq 50\%$ at the higher incident ion energies.[8]

In the present work, a similar behavior has been observed between the calculated PWBA-BC and the experimentally determined cross sections at the higher velocities—the difference becoming larger for greater Z_1/Z_2 ratios, as expected. An inherent assumption in the theories of direct Coulomb ionization is that $Z_1/Z_2 \ll 1$. Figure 1 presents a representative sample of the x-ray production cross sections determined in the present work. Experimental x-ray production cross sections for ^{14}N ion bombardment of Ca, Ti, Co, and Zn are compared to the theoretical predictions of the BEA,[37] and the modified PWBA.[9,10] The theoretical K-shell ionization cross sections are compared to the experimental x-ray production cross sections using fitted values of the fluorescence yields for single-hole ionization taken from Bambynek *et al.*[40]

The BEA and PWBA predictions, as shown in Fig. 1, overestimate the experimental cross sections at the lower velocities by approximately a factor of 10. The BEA and PWBA calculations do not exhibit the energy dependence of the data. The PWBA-BC predictions are much lower than those of the PWBA. While only slightly underestimating the experimental values at the lower energies by ~10% for all elements, the PWBA-BC underestimates the data at higher energies by 75% for Ca, 70% for Ti, 44% for Co, and 41% for Zn. The

TABLE III. Experimental K-shell x-ray production cross sections, $K\beta/K\alpha$ x-ray intensity ratios, and $K\alpha$ and $K\beta$ x-ray energy shifts for ^{14}N ion bombardment.[a]

Element	E (MeV)	σ_K (b)	$K\beta/K\alpha$	$\Delta E_{K\alpha}$ (eV)	$\Delta E_{K\beta}$ (eV)	Element	E (MeV)	σ_K (b)	$K\beta/K\alpha$	$\Delta E_{K\alpha}$ (eV)	$\Delta E_{K\beta}$ (eV)
$_{20}$Ca	7.0	61.2	0.105	48	102	$_{25}$Mn	7.0	13.4	0.125	34	88
	8.4	150	0.128	60	156		8.4	27.6	0.132	36	109
	9.8	394	0.132	59	154		9.8	52.6	0.142	40	122
	12.6	1340	0.138	62	157		12.6	136	0.150	48	143
	15.4	3610	0.141	65	174		15.4	366	0.159	53	151
	18.2	7200	0.140	62	189		18.2	757	0.162	57	162
	21.0	10 000	0.143	61	158		21.0	1330	0.163	58	167
	23.8	15 500	0.139	61	173		23.8	1820	0.166	59	174
	26.6	23 700	0.141	64	145		26.6	3430	0.163	59	165
	29.4	30 200	0.139	60	148		29.4	4550	0.163	58	156
	32.2	34 400	0.140	63	158		32.2	5890	0.163	57	157
	35.0	36 500	0.136	54	123		35.0	7810	0.162	55	157
$_{22}$Ti	7.0	40.2	0.100	46	98	$_{26}$Fe	7.0	9.71	0.125	26	98
	8.4	90.2	0.137	49	141		8.4	19.0	0.133	32	108
	9.8	170	0.142	54	146		9.8	34.6	0.140	36	121
	12.6	504	0.146	59	158		12.6	99.2	0.150	43	139
	15.4	1470	0.152	65	171		15.4	235	0.158	49	152
	18.2	2910	0.155	74	157		18.2	532	0.163	52	162
	21.0	4420	0.152	62	175		21.0	951	0.167	54	166
	23.8	6790	0.155	60	170		23.8	1470	0.165	52	165
	26.6	10 600	0.151	60	159		26.6	2240	0.166	55	165
	29.4	13 800	0.152	60	145		29.4	3260	0.166	54	163
	32.2	17 800	0.157	58	140		32.2	4040	0.168	52	155
	35.0	20 300	0.149	56	141		36.0	5640	0.161	52	152
$_{23}$V	7.0	28.8	0.116	47	113	$_{27}$Co	12.6	73.2	0.151	38	119
	8.4	60.0	0.133	46	119		15.4	167	0.149	44	145
	9.8	111	0.139	49	138		18.2	329	0.166	47	159
	12.6	333	0.151	55	154		21.0	551	0.176	50	159
	15.4	856	0.154	59	163		23.8	947	0.172	51	157
	18.2	1780	0.156	58	165		26.6	1510	0.170	51	159
	21.0	2880	0.156	57	165		29.4	2190	0.174	50	154
	23.8	4700	0.160	58	162		32.2	2920	0.171	50	154
	26.6	7140	0.158	57	155		35.0	3690	0.166	51	154
	29.4	8270	0.156	56	150						
	32.2	12 300	0.157	55	146						
	35.0	14 900	0.156	55	147						
$_{24}$Cr	7.0	21.1	0.122	39	103	$_{28}$Ni	7.0	5.59	0.132	23	97
	8.4	40.8	0.134	43	115		8.4	11.6	0.137	24	96
	9.8	78.9	0.140	45	125		9.8	20.3	0.146	30	110
	12.6	220	0.150	51	148		12.6	49.4	0.151	39	124
	15.4	558	0.156	56	155		15.4	122	0.159	44	145
	18.2	1020	0.166	56	160		18.2	250	0.163	49	153
	21.0	1540	0.159	56	161		21.0	439	0.167	52	167
	23.8	3270	0.163	55	186		23.8	681	0.174	53	170
	26.6	4650	0.163	57	153		26.6	1090	0.174	56	168
	29.4	6410	0.166	56	151		29.4	1590	0.170	55	167
	32.2	8100	0.163	54	141		32.2	2090	0.171	54	162
	35.0	9720	0.164	52	137		36.0	2990	0.170	54	160

TABLE III. (*continued*)

Element	E (MeV)	σ_K (b)	$K\beta/K\alpha$	$\Delta E_{K\alpha}$ (eV)	$\Delta E_{K\beta}$ (eV)	Element	E (MeV)	σ_K (b)	$K\beta/K\alpha$	$\Delta E_{K\alpha}$ (eV)	$\Delta E_{K\beta}$ (eV)
$_{29}$Cu	7.0	4.35	0.143	20	89	$_{30}$Zn	7.0	2.97	0.128	14	102
	8.4	8.82	0.141	23	101		8.4	6.12	0.153	13	108
	9.8	15.6	0.144	26	106		9.8	11.5	0.163	15	124
	12.6	39.6	0.154	35	134		12.6	30.5	0.156	24	131
	15.4	86.1	0.158	39	141		15.4	62.7	0.168	31	142
	18.2	177	0.168	45	151		18.2	125	0.171	33	146
	21.0	294	0.171	48	162		21.0	201	0.174	41	162
	23.8	489	0.174	51	168		23.8	345	0.178	44	170
	26.6	801	0.176	53	170		26.6	547	0.180	47	170
	29.4	1140	0.174	52	167		29.4	778	0.179	48	167
	32.2	1580	0.175	52	163		32.2	1150	0.180	48	167
	35.0	1980	0.173	51	160		36.0	1690	0.179	48	165
	36.0	2310	0.177	52	156						

[a] The absolute uncertainties associated with the measured values are discussed in the text and in Ref. 8.

majority of the correction for binding energy and Coulomb deflection is due to the binding-energy effect. The correction for Coulomb deflection, though quite small in magnitude has been included in the calculations. The Coulomb deflection correction for the heaviest elements studied in the present work, Zn, was only 2.5% of the total correction for binding energy and Coulomb deflection at the lowest energy. The approximate relativistic correction, which was significant only at the lower velocities, was included in the calculations. The relativistic corrections at the lowest energy of interest, 7 MeV, were 2.6% for Ca, 4.6% for Ti, and 21% for Zn. The inclusion of the high-velocity polarization and relativistic corrections (PWBA-BCPR in Fig. 1) improves the agreement between experiment and theory at higher velocities.

One observes, according to Fig. 1, that even for the fully modified PWBA there exists a systematic deviation of the theoretical calculations from the data which becomes larger as the ratio of Z_1/Z_2 increases. This can perhaps be seen more easily in the form of a universal plot. If the PWBA formalism is an accurate description of the ionization process the measured cross sections should exhibit a universal behavior for all values of the variables η_K and θ_K when scaled by the Coulomb deflection correction, the relativistic correction (R), the fluorescence yield (ω_0) and ($\sigma_{0K}/\zeta\theta_K$).

Figure 2 presents an experimentally inferred, F^{expt}, given by

$$F\left[\frac{\eta_K}{\zeta^2\theta_K^2}\right]^{\text{expt}} = \frac{\sigma_{K_x}^{\text{expt}}}{R\omega_0 9E_{10}(b\zeta\theta_K\eta_K^{-3/2})(\sigma_{0K}/\zeta\theta_K)} . \quad (9)$$

The solid line in Fig. 2 is the theoretical universal function, $F(\eta_K/\zeta^2\theta_K^2)$. The experimental data fall on a universal curve within statistics, but not on the theoretical universal curve given by the solid line. The experimental data are underestimated by $\lesssim 10\%$ for values of $\eta_K/\zeta^2\theta_K^2 < 0.1$. For values of $\eta_K/\zeta^2\theta_K^2 > 0.1$, the experimental data and the theory are in poor agreement—with the difference increasing for larger values of $\eta_K/\zeta^2\theta_K^2$. The disagreement can be partially explained by changes in the K-shell fluorescence yield due to multiple ionization.

For comparisons between experiment and theory, ω_0 for single-hole ionization has been used. These values of ω_0 are not appropriate due to the large amounts of multiple ionization that are present during the heavy ion-atom collision. Multiple ionization has been shown to produce shifts in the energies of x-ray transitions and changes in x-ray intensity ratios. Figure 3 presents measured x-ray energy shifts for $K\alpha$ and $K\beta$ x-ray transitions for Ca, Mn, and Zn. Since the maximum K x-ray energy shifts occur where the ratios of the projectile velocity (v_1) to the average L-shell electron velocity ($\bar{v}_L$) are close to one, the majority of the K x-ray energy shifts may be attributed to multiple L-shell ionization. In order to be able to estimate the changes in the fluorescence yields due to multiple ionization, we have employed the scaling law of Larkins.[41] We have calculated the changes in the fluorescence yields for the defect configuration by scaling the radiative and Auger transition rates given by McGuire[42] by the fraction of the number of $2p$ electrons present in the L shell. Considering the approximations present in these calculations, we have made the

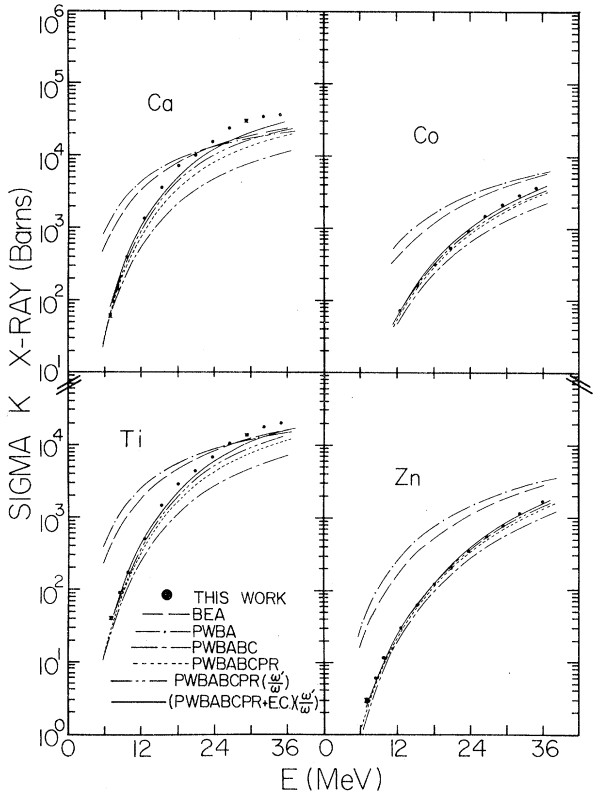

FIG. 1. K-shell x-ray production cross sections for ^{14}N ion bombardment of thin solid targets of Ca, Ti, Co, and Zn. The experimental data are compared to the predictions of the BEA, the PWBA, the PWBA with binding energy (B), Coulomb deflection (C), target electron polarization (P), and relativistic effects (R) employing single-hole fluorescence yields. Corrections for changes in the fluorescence yields due to multiple ionization (ω/ω') have been applied to the fully modified PWBA, PWBA-BCPR. Electron capture (EC) contributions have been added to the above direct ionization calculations.

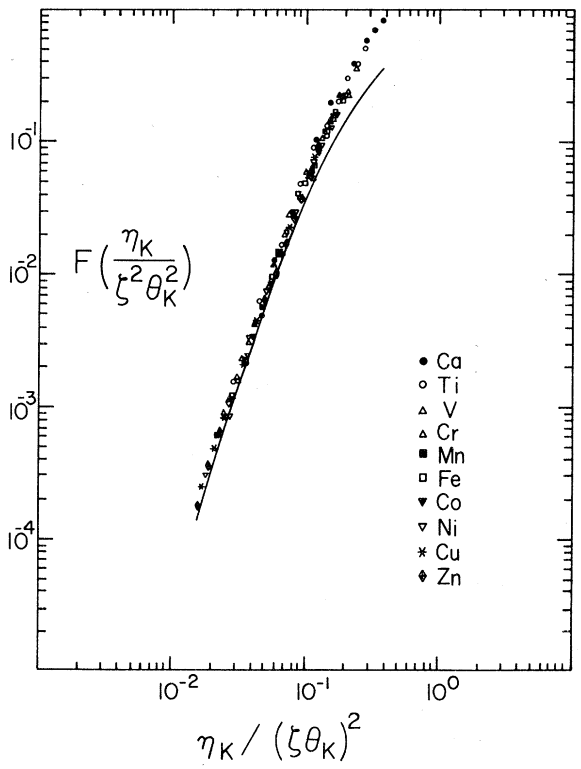

FIG. 2. Experimental x-ray production cross sections for ^{14}N ion impact scaled as a function of $\eta_K/\zeta^2\theta_K^2$ for comparison to the approximate universal function, $F(\eta_K/\zeta^2\theta_K^2)$, in the PWBA theory of Basbas *et al.* (Refs. 9 and 10). The experimentally inferred function $F(\eta_K/\zeta^2\theta_K^2)^{\text{expt}}$, is given in the text and does not include changes in the fluorescence yields due to multiple ionization which are given in Table IV. The theoretical universal function is represented by the solid line.

additional assumption that the energy shifts are due entirely to $2p$ vacancies and have neglected $2s$, $3s$, and $3p$ vacancies. The number of $2p$ electrons present were estimated at a number of different incident energies by comparing the measured $K\alpha$ and $K\beta$ energy shifts with those calculated by Hartree-Fock-Slater techniques.[43]

Table IV presents ratios of the fluorescence yields calculated by the above method to those calculated for the no defect configuration for a number of representative elements. The maximum fluorescence yield corrections determined for Ca and Zn correspond approximately to three and two $2p$ vacancies, respectively. The PWBA-BCPR calculations including the fluorescence yield corrections are shown in Fig. 1. Agreement between theory and experiment is improved but a discrep-

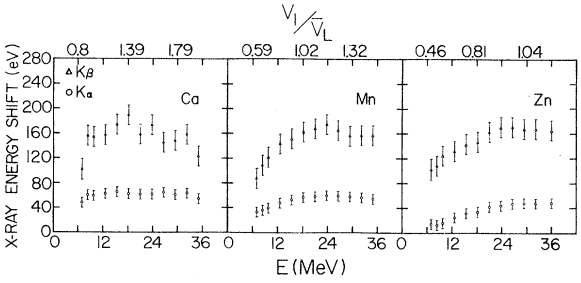

FIG. 3. X-ray energy shifts for $K\alpha$ and $K\beta$ transitions for ^{14}N ion bombardment of Ca, Mn, and Zn. The maximum energy shift is observed to occur where the ratios of the projectile velocity (v_1) to the average L-shell electron velocity ($\bar{v}_L$) are close to one, indicating that the majority of the K x-ray energy shifts may be attributed to multiple L-shell ionization. $v_1/\bar{v}_L = (E/\lambda\bar{U}_L)^{1/2}$, where E is the incident ^{14}N ion energy, λ is the ratio of ^{14}N mass to electron mass, and $\bar{U}_L = \frac{1}{4}(U_{L_1} + U_{L_2} + 2U_{L_3})$ is the average L-shell electron binding energy.

TABLE IV. Ratios of the fluorescence yield calculated for multiple $2p$ vacancies to the fluorescence yield calculated for the no-defect configuration.

E (MeV) \ ω_0[a]	$_{20}$Ca 0.163	$_{22}$Ti 0.219	$_{23}$V 0.250	$_{27}$Co 0.381	$_{30}$Zn 0.479
7.0	1.20	1.15	1.14		1.06
12.6	1.27	1.20	1.17	1.08	1.08
18.2	1.28	1.22	1.18	1.10	1.08
23.8	1.28	1.21	1.18	1.10	1.10
29.4	1.26	1.20	1.17	1.10	1.09
35.0	1.22	1.19	1.17	1.10	1.09

[a] Numerical values of the fluorescence yield for single hole ionization, ω_0, are taken from the fitted values of Bambynek *et al.* (Ref. 40).

ancy still exists for the light targets at the higher energies. In Fig. 2, the inclusion of fluorescence yield corrections would remove the ~10% disagreement, discussed earlier, between the experimental data and the universal curve for values of $\eta_K/\zeta^2\,\theta_K^2 \leq 0.1$. For values of $\eta_K/\zeta^2\theta_K^2 > 0.1$, the agreement between experimental data and the universal curve would be improved. The difference becomes larger as the ratio of Z_1/Z_2 becomes larger which may be an indication of the presence of ionization processes other than direct Coulomb ionization.

For heavier projectiles, K-electron transfer to bound states of the projectile may be important to K-vacancy production in the target.[19-21] Recently, this has been shown by Hopkins[22] and Gray *et al.*[23] to produce large enhancements in the target cross sections which are a strong function of target thicknesses for Cl projectiles.

Target thickness effects produce residual excitation of projectile K-shell electrons due to multiple collisions in the solid. The fraction of projectiles with K vacancies can be larger than fractions determined outside the solid. For ^{14}N ion bombardment of the elements investigated in the present work, we do not expect target thickness effects to be a major consideration in view of the universality of the entire set of experimental data exhibited in Fig. 2 for the range of target thicknesses employed (12–80 μg/cm^2). We estimate these target thickness effects to be negligible for the heavier elements studied and <10% for the lightest elements. To provide as complete a picture as possible, we have also included theoretical calculations of electron capture processes for the present results.

Theoretical calculations of inner-shell ionization through K electron capture (EC) by heavy charged particles have recently been reported by Lapicki and Losonsky.[44] They employ the analytical expressions of Nikolaev[45] with screened hydrogenic wave functions in the Oppenheimer,[46] Brinkman-Kramers approximation[47] and include modifications for increased binding energy and Coulomb deflection effects in a fashion similar to that used for direct ionization by Basbas *et al.*[9,10]

The solid lines in Fig. 1 are theoretical calculations including direct ionization (PWBA-BCPR) +EC contributions with the fluorescence yield modification (ω'/ω). The EC contributions presented in Fig. 1 have been determined by weighting the EC calculations of Lapicki and Losonsky[44] for individual incident charge states by the equilibrium charge-state fractions for ^{14}N ions exiting from solids.[48] This procedure assumes that charge-state equilibrium has been reached by the ^{14}N ions in passing through the target thicknesses presented in Table I and that these equilibrium distributions outside the solids are good representations of actual charge-state distributions in the solid. This seems reasonable since at equilibrium, 98% of the incident 35 MeV-^{14}N ions have 1 or 2 K vacancies.[48] The addition of K-shell EC contributions provides excellent agreement between experiment and theory for the heavier elemental targets. The theoretical calculations, while providing excellent agreement between experiment and theory at lower velocities, underestimate the experimental cross sections at higher velocities by increasing amounts for larger values of Z_1/Z_2 approaching 25% for Ca. This disagreement at the higher energies may be partially due to the use of an analytic representation for the function, $F(\eta_K/\zeta^2\theta_K^2)$, in the PWBA formalism and to uncertainties in the equilibrium charge state fractions[48] used to weight the EC calculations.[44]

VI. CONCLUSIONS

The purpose of the present work is to make comparisons between experiment and theory of inner-shell ionization for ranges of the parameters Z_1/Z_2 and v_1/v_e where Coulomb ionization should be the primary excitation mechanism. The work has shown that theories of Coulomb ionization are quite applicable for the present work and can be extended to values of $Z_1/Z_2 \lesssim 0.35$ if the effects of increased electron binding, Coulomb deflection, polarization, and relativistic electron velocities are included. The binding-energy effect was found to be the dominant correction which removed the majority of the discrepancy between experiment and theory. The correction for target electron polarization improved considerably the agreement at higher velocities. The corrections for Coulomb deflection and relativistic effects

were found to be small but significant for the ranges of Z_1/Z_2 and v_1/v_e in this work. There is need for further theoretical work concerning relativistic effects and the tables of the universal functions, F, which need to be extended for larger values of θ_K.

The importance of changes in the fluorescence yields due to multiple ionization effects and the inclusion of electron-capture contributions are noted to improve the comparison between experiment and theory for heavy-ion bombardment.

ACKNOWLEDGMENTS

The authors wish to acknowledge R. P. Chaturvedi, R. Wheeler, J. Lin, K. Kuenhold. S. Cipolla, J. Tricomi, A. D. Ray, S. Wilson, J. Rowe, L. Hawthorne, and F. Elliott for their assistance with the data acquisition. A particular thanks goes to C. D. Moak, W. T. Milner, E. Richardson, and R. P. Cumby of Oak Ridge National Laboratory for their invaluable assistance with the experimental facilities of the Tandem Accelerator Laboratory. We would like to thank George Basbas for providing us with computer codes to calculate the modified PWBA with polarization contributions and G. Lapicki for providing the electron-capture calculations prior to publication. We would like to thank Tom Gray for helpful comments concerning the determination of fluorescence yields for defect configurations, and Walter Meyerhof for helpful discussions concerning molecular orbital and recoil effects.

---

*Experiments performed at Oak Ridge National Laboratory Tandem Van de Graaff facility which is supported by ERDA.and operated by Union Carbide Corporation.

†Supported by the NTSU Faculty Research Fund, the Robert A. Welch Foundation, and the Research Corporation. Travel for participants was provided by Oak Ridge Associated Universities through contractual arrangement with ERDA.

[1]See for example, D. H. Madison, and E. Merzbacher, *Atomic Inner-Shell Processes*, edited by Bernd Crasemann (Academic, New York, 1975), Vol. 1, p. 1.

[2]U. Fano and W. Lichten, Phys. Rev. Lett. 14, 627 (1965); M. Barat and W. Lichten, Phys. Rev. A 6, 211 (1972).

[3]See for example, Fig. 13 of Ref. 1.

[4]J. D. Garcia, E. Gerjuoy, and J. W. Welker, Phys. Rev. 165, 66 (1968); J. D. Garcia, Phys. Rev. A 1, 1402 (1970); 1, 280 (1970).

[5]E. Merzbacher and H. Lewis, *Encyclopedia of Physics*, edited by S. Flügge (Springer-Verlag, Berlin, 1958), Vol. 34, p. 166.

[6]J. D. Garcia, R. J. Fortner, and T. M. Kavanagh, Rev. Mod. Phys. 45, 111 (1973).

[7]F. D. McDaniel, T. J. Gray, and R. K. Gardner, Phys. Rev. A 11, 1607 (1975).

[8]F. D. McDaniel, T. J. Gray, R. K. Gardner, G. M. Light, J. L. Duggan, H. A. Van Rinsvelt, R. D. Lear, G. H. Pepper, J. W. Nelson, and A. R. Zander, Phys. Rev. A 12, 1271 (1975).

[9]G. Basbas, W. Brandt, and R. Laubert, Phys. Rev. A 7, 983 (1973).

[10]G. Basbas, W. Brandt, and R. Laubert (private communications).

[11]G. Basbas, W. Brandt, R. Laubert, and A. Schwarzschild, Phys. Rev. Lett. 27, 171 (1971).

[12]G. Basbas, W. Brandt, and R. Laubert, Phys. Rev. Lett. 34A, 277 (1971).

[13]K. W. Hill and E. Merzbacher, Phys. Rev. A 9, 156 (1974).

[14]J. Tricomi, J. L. Duggan, F. D. McDaniel, P. D. Miller, R. P. Chaturvedi, R. M. Wheeler, J. Lin, K. A. Kuenhold, L. A. Rayburn, S. J. Cipolla, Phys. Rev. A (to be published).

[15]G. Bissinger, P. H. Nettles, S. M. Shafroth, and A. W. Waltner, Phys. Rev. A 10, 1932 (1974).

[16]D. Jamnik and C. Zupancic, Mat. Fys. Medd. Dan. Vid. Selsk. 31, No. 2 (1957).

[17]B. H. Choi, Phys. Rev. A 4, 1002 (1971).

[18]J. S. Hansen, Phys. Rev. A 8, 822 (1973).

[19]J. R. Macdonald, P. Richard, C. L. Cocke, M. Brown, and I. A. Sellin, Phys. Rev. Lett. 31, 684 (1973); L. M. Winters, J. R. Macdonald, M. D. Brown, T. Chiao, L. D. Ellsworth, and E. W. Pettus, Phys. Rev. A 8, 1835 (1973); M. D. Brown, L. D. Ellsworth, J. A. Guffey, T. Chiao, E. W. Pettus, L. M. Winters, and J. R. Macdonald, Phys Rev. A 10, 1255 (1974).

[20]J. R. Mowat, D. J. Pegg, R. S. Peterson, P. M. Griffin, and I. A. Sellin, Phys. Rev. Lett. 29, 1577 (1972).

[21]A. M. Halpern and J. Law, Phys. Rev. Lett. 31, 4 (1973); J. H. McGuire, Phys. Rev. A 8, 2760 (1973).

[22]F. Hopkins, Phys. Rev. Lett. 35, 270 (1975).

[23]T. J. Gray, P. Richard, K. A. Jamison, J. M. Hall, and R. K. Gardner, Phys. Rev. A 14, 1333 (1976).

[24]W. E. Meyerhof, Phys. Rev. Lett. 31, 1341 (1973); W. E. Meyerhof, Phys. Rev. A 10, 1005 (1974); W. E. Meyerhof, T. K. Saylor, S. M. Lazarus, A. Little, R. Anholt, L. F. Chase, Jr., Proceedings of the Second International Conference on Inner Shell Ionization Phenomena, Freiburg, Germany, 1976.

[25]N. Cue, V. Dutkiewicz, P. Sen, H. Bakhru, Phys. Rev. Lett. 32, 1155 (1974).

[26]F. D. McDaniel and J. L. Duggan, *Proceedings of the Fourth International Conference on Beam Foil Spectroscopy and Heavy Ion Atomic Physics, Gatlinburg, Tenn., 1975*, edited by I. Sellin and D. Pegg (Plenum, New York, 1976) Vol. 2, p. 519; F. D. McDaniel, J. L. Duggan, J. Tricomi, P. D. Miller, K. A. Kuenhold, F. Elliott, J. Lin, R. M. Wheeler, and R. P. Chaturvedi, Bull. Am. Phys. Soc. 21, 650 (1976).

[27]L. B. Magnusson, Phys. Rev. 107, 161 (1957); R. J. Gehrke and R. A. Lokken, Nucl. Instrum. Methods 97, 219 (1971); J. S. Hansen, J. C. McGeorge, D. Nix, W. D. Schmidt-Ott, I. Unus, and R. W. Fink, Nucl. Instrum. Methods 106, 365 (1973); W. J. Gallagher and S. J. Cipolla, Nucl. Instrum. Methods 122, 405 (1974); J. L. Campbell and L. A. McNelles, Nucl. Instrum. Methods, 117, 519 (1974); 125, 205 (1975).

[28]J. J. Simpson, J. A. Cookson, D. Ecclesmall, and

M. O. L. Yates, Nucl. Phys. 62, 385 (1965); A. W. Obst, D. L. McShan, and R. H. Davis, Phys. Rev. C 6, 1814 (1972).
[29]R. Laubert, H. Haselton, J. R. Mowat, R. S. Peterson, and I. A. Sellin, Phys. Rev. A 11, 135 (1975).
[30]E. M. Berstein and H. W. Lewis, Phys. Rev. 95, 83 (1954); C. W. Lewis, R. L. Watson, and J. B. Natowitz, Phys. Rev. A 5, 1773 (1972); L. M. Middleman, R. L. Ford, and R. Hofstadter, Phys. Rev. A 2, 1429 (1970); E. H. Pedersen, S. J. Czuchlewski, M. D. Brown, L. D. Ellsworth, and J. R. Macdonald, Phys. Rev. A 11, 1267 (1975).
[31]K. Taulbjerg and P. Sigmund, Phys. Rev. A 5, 1285 (1976).
[32]K. Taulbjerg, B. Fastrup, and E. Laegsgaard, Phys. Rev. A 8, 1814 (1973).
[33]W. Brandt and R. Laubert, Phys. Lett. 43A, 53 (1973).
[34]D. Burch and K. Taulbjerg, Phys. Rev. A 12, 508 (1975).
[35]G. S. Khandelwal, B. H. Choi, and E. Merzbacher, At. Data 1, 103 (1969).
[36]W. Brandt and G. Lapicki, Phys. Rev. A 10, 474 (1974).
[37]J. H. McGuire and P. Richard, Phys. Rev. A 8, 1374 (1973).
[38]B. K. Thomas and J. D. Garcia, Phys. Rev. 179, 94 (1969).
[39]T. J. Gray, P. Richard, R. L. Kauffman, T. C. Holloway, R. K. Gardner, G. M. Light, and J. Guertin, Phys. Rev. A 13, 1344 (1976).
[40]W. Bambynek, B. Craseman, R. W. Fink, H. U. Freund, H. Mark, C. D. Swift, R. E. Price, and P. V. Rao, Rev. Mod. Phys. 44, 716 (1972).
[41]F. P. Larkins, J. Phys. B 4, L29 (1971).
[42]E. J. McGuire, Phys. Rev. A 2, 273 (1970).
[43]F. Herman and S. Skillman, *Atomic Structure Calculations* (Prentice-Hall, Englewood Cliffs, N. J., 1963).
[44]G. Lapicki and W. Losonsky, Bull. Am. Phys. Soc. 21, 32 (1976); this issue, Phys. Rev. A 15, 896 (1977); G. Lapicki (private communications).
[45]V. S. Nikolaev, Zh. Eksp. Teor. Fiz. 51, 1263 (1966) [Sov. Phys. -JETP 24, 847 (1967)].
[46]J. R. Oppenheimer, Phys. Rev. 31, 349 (1928).
[47]H. C. Brinkman and H. A. Kramers, Proc. Acad. Sci. (Amsterdam) 33, 973 (1930).
[48]J. B. Marion and F. C. Young, *Nuclear Reaction Analysis* (North Holland, Amsterdam, 1968), p. 34.